

Investigating Transient Responses of IEEE 6 Bus Power System to Various Fault Types using PowerWorld Simulator

Sami Melih Öztürk ^a, Ahmet Çifci ^{b,1}

^a Graduate School of Natural and Applied Sciences, Burdur Mehmet Akif Ersoy University, Burdur, Türkiye
ORCID ID: 0009-0009-9054-7483

^b Department of Electrical and Electronics Engineering, Burdur Mehmet Akif Ersoy University, Burdur, Türkiye
ORCID ID: 0000-0001-7679-9945

Abstract

Transient analysis of power systems is essential for understanding dynamic responses and stability under fault conditions. This paper focuses on the transient analysis of the IEEE 6 bus power system using the PowerWorld Simulator, with the primary objective of investigating the system's behavior under various fault conditions, including three-phase balanced faults, line-to-ground faults, line-to-line faults, and double line-to-ground faults. The IEEE 6 bus system, a standardized benchmark for testing power system algorithms, provides a simplified yet effective model for examining transient phenomena. Utilizing the PowerWorld Simulator, this study models and simulates fault conditions to assess their impacts on key parameters such as bus voltages, generator rotor angles, and generator voltages. By conducting a series of simulations, we aim to provide a detailed characterization of the transient response of the IEEE 6 bus system under each fault scenario. The results of our analysis reveal distinct patterns of system behavior for each type of fault. Three-phase balanced faults, being the most severe, significantly disrupt system stability, causing considerable deviations in voltage and phase angles. Line-to-ground faults, although less severe, still pose substantial challenges, especially in terms of voltage stability at the faulted bus. Line-to-line faults primarily affect the phase voltages, leading to asymmetrical disturbances that propagate through the network. Double line-to-ground faults, which combine characteristics of line-to-line and line-to-ground faults, exhibit complex transient dynamics that test system resilience and control mechanisms. Our findings underscore the necessity for robust protective measures and control strategies to mitigate the adverse effects of these faults. The study highlights the importance of fault location, fault type, and system configuration in determining the overall stability and reliability of the power system.

Keywords: “Fault analysis, IEEE 6 bus system, PowerWorld simulator, transient stability.”

1. Introduction

In electrical power systems, faults can disrupt normal operation, cause equipment damage, and pose safety hazards. The four main types of faults are line-to-ground, line-to-line, double line-to-ground, and three-phase balanced faults. Line-to-ground faults occur when one phase conductor contacts the ground or a grounded object, creating an imbalance in the system [1]. This is the most common fault type, characterized by high fault currents flowing from the line to the ground, potentially causing equipment damage and power outages. Causes include insulation failure, physical damage, or environmental factors. Line-to-line faults occur when two phase conductors come into contact, leading to an unbalanced condition with high fault currents between the phases [2]. This can result from insulation failure, swaying conductors in high winds, or mechanical damage, posing risks of extensive equipment damage and arc flash incidents. Double line-to-ground faults involve two phase conductors contacting the ground simultaneously, causing severe imbalance and high fault currents [3]. These faults, often due to insulation failure or severe environmental conditions, can lead to extensive system damage and pose greater safety hazards. Three-phase balanced faults, also known as symmetrical faults, involve all three phases short-circuiting together, resulting in extremely high fault currents [4]. Although less common, these faults are the most severe, potentially causing maximum equipment damage and widespread power outages due to their catastrophic nature, including major equipment explosions or extreme mechanical damage. Understanding these fault types and implementing effective detection and protection mechanisms is crucial for maintaining power system stability and safety.

In recent years, the use of simulation tools in power system analysis has become increasingly prevalent [5]. The increasing prominence of simulation tools in power system analysis reflects the growing complexity and dynamic nature of modern power

¹ Corresponding Author
E-mail Address: acifci@mehmetakif.edu.tr

systems. Among these tools, the PowerWorld Simulator stands out as a powerful software package that offers a comprehensive platform for studying and analyzing various aspects of power systems [6-8]. Many researchers have explored the application of PowerWorld Simulator in various aspects of power system analysis, including load flow studies, contingency analysis, and dynamic simulations [9-11].

One of the key areas where PowerWorld Simulator has been extensively utilized is in the analysis of transient stability in power systems. Transient stability is a critical concern in power system operation, as it determines the system's ability to withstand sudden disturbances, such as faults or load changes, and maintain synchronism [12]. By simulating the system's response to various transient events, researchers and practitioners can gain valuable insights into system behavior and devise effective strategies for system protection and control. Several studies have investigated the use of PowerWorld Simulator in transient stability analysis, focusing on different power system configurations and scenarios. Kaur and Kumar [13] concentrated on enhancing transient stability in the IEEE 9 bus system through the PowerWorld Simulator, emphasizing the importance of bolstering transient stability in power systems. Similarly, Mahasathyavathi et al. [14] explored load frequency control for a multi-area power system using the PowerWorld Simulator, stressing the significance of minimizing transient response and assessing generator contributions under different disturbances. These studies underscore the pivotal role of PowerWorld Simulator in scrutinizing and enhancing power system performance under transient conditions. Furthermore, Kim and Overbye [15] introduced an optimal subinterval selection approach for power system transient stability simulation, showcasing the versatility of PowerWorld Simulator in managing intricate analyses related to transient stability. Additionally, Demetriou et al. [16] executed dynamic tests on IEEE test systems for transient analysis, further demonstrating the applicability of simulation tools like PowerWorld in evaluating power system conditions post-contingency events. Summaries of other studies on transient stability analysis using PowerWorld Simulator are provided in Table 1.

Table 1. List of studies on transient stability analysis using PowerWorld Simulator.

Author(s)	Publication Year	Summary
Anuar et al. [17]	2020	This paper explores transient stability analysis of the IEEE 14 bus system using PowerWorld Simulator, with detailed observations and outcomes.
Anwar et al. [18]	2020	The paper focuses on evaluating the transient stability of the IEEE 9 bus system when subjected to various simultaneous disturbances.
Patel [19]	2020	The paper presents a method for enhancing the transient stability of a three-machine nine-bus power system by tuning power system stabilizers using a frequency response approach.
Tina et al. [20]	2021	The paper evaluates various methods for enhancing transient stability in power systems, focusing on their technical effectiveness and economic feasibility.
Rajesh Varma et al. [21]	2021	This paper investigates the transient stability of the IEEE 9 bus power system, focusing on the system's response to various disturbances using the PowerWorld Simulator.
Tina et al. [22]	2022	This paper examines various technical strategies aimed at enhancing the transient stability of power systems that integrate wind power generation.
Salim et al. [23]	2023	This paper examines the transient stability of a power system under different contingency scenarios, using PowerWorld Simulator to analyze the impact of faults and load changes on system stability and synchronism.

The IEEE 6 bus system, a widely accepted benchmark for power system studies, was chosen for its simplicity and representativeness of key features found in larger systems. This small-scale, radial power system allows for efficient analysis of transient phenomena without excessive complexity. By leveraging the capabilities of PowerWorld Simulator, this study aims to contribute to the field by specifically focusing on transient behavior within the IEEE 6 bus power system. While previous research has explored transient stability in larger systems, the IEEE 6 bus system presents a unique challenge due to its smaller scale and potentially different transient response characteristics. Most studies concentrate on larger, more complex networks. This research will address this gap by conducting a comprehensive transient analysis of the IEEE 6 bus system using PowerWorld. By simulating various transient events, such as fault occurrences, the study will provide valuable insights into the system's dynamic behavior and assess its performance under different operating conditions. The insights gained from these simulations can be applied to larger systems, contributing to a deeper understanding of power system dynamics and stability. The main contribution of this study can be summarized in the following points:

- Transient analysis helps identify potential vulnerabilities, stability issues, and system responses to disturbances. These are essential for ensuring the reliability and resilience of power networks.
- The findings from this study can be used to develop and validate control strategies, protection schemes, and mitigation techniques that can be applied to larger-scale power systems with similar characteristics.
- This work can contribute to the broader understanding of power system dynamics and support the development of more robust and efficient power system designs and operation practices.

The rest of the paper is structured as follows. Section 2 describes the IEEE 6 bus system, a standard test system used in power system analysis, and the application of the Newton-Raphson method for power flow analysis. Section 3 presents the simulation

results for each fault type, analyzing the effects on bus voltages, generator rotor angles, and generator voltages. Finally, Section 4 synthesizes the principal findings of the study, elucidates their significance and possible applications, and offers recommendations for future research directions.

2. Power System Modeling

This study utilizes the IEEE 6 bus power system. The IEEE 6 bus power system is a standard test system used in power system analysis and evaluation. It is a simplified representation of a real power grid, consisting of six buses, three generators, three loads, and eleven transmission lines. This system is designed to provide a common platform for studying various power system phenomena and testing different power system applications. The single line diagram of IEEE 6 bus power system is shown in Fig. 1.

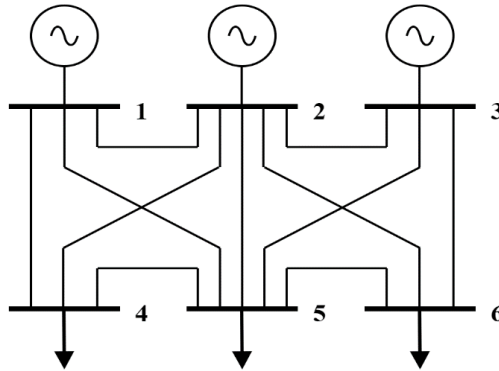


Fig. 1. IEEE 6 bus power system.

Bus 1 is a slack bus. This bus acts as the reference bus, providing a constant voltage magnitude (in per-unit, pu) and angle. It balances the active and reactive power in the system. Buses 2 and 3 are generator buses. These are also known as PV buses. They have a fixed voltage magnitude, but their voltage angle and real power output can vary. Buses 4, 5, and 6 are load buses. These are also known as PQ buses. They have specific power demands (active and reactive power) that need to be met by the generators. The bus data and line parameters for the IEEE 6 bus power system are provided in Table 2 and Table 3, respectively.

Table 2. Bus data of IEEE 6 bus system.

Bus No	Bus Type	Voltage (pu)	Generation		Load	
			P (MW)	Q (MVA _r)	P (MW)	Q (MVA _r)
1	Slack	1.05	-	-	0	0
2	PV	1.05	50	-	0	0
3	PV	1.07	60	-	0	0
4	PQ	1	0	0	70	70
5	PQ	1	0	0	70	70
6	PQ	1	0	0	70	70

Table 3. Line parameters of IEEE 6 bus system.

Bus No From-To	Resistance (pu)	Reactance (pu)	Line Charging (pu)
1-2	0.1	0.2	0.04
1-4	0.05	0.2	0.04
1-5	0.08	0.3	0.06
2-3	0.05	0.25	0.06
2-4	0.05	0.1	0.02
2-5	0.1	0.3	0.04
2-6	0.07	0.2	0.05
3-5	0.12	0.26	0.05
3-6	0.02	0.1	0.02
4-5	0.2	0.4	0.08
5-6	0.1	0.3	0.06

The power flow analysis of the IEEE 6 bus power system modeled in PowerWorld Simulator was performed using the Newton-Raphson method. The Newton-Raphson method, a powerful iterative technique, finds widespread application in power flow analysis. This method leverages the Taylor series expansion to linearize the nonlinear power flow equations, thereby

transforming them into a system of linear equations that can be readily solved [7]. Starting with an initial guess for the voltage magnitudes and angles at each bus, the Newton-Raphson method iteratively refines these estimates by solving the linearized equations [24]. The process continues until the difference between successive iterations falls below a predetermined tolerance, signifying convergence to a solution. The robustness and rapid convergence of the method establish it as a fundamental tool in power system analysis, facilitating engineers in precisely predicting the steady-state operating conditions of electrical networks. The power flow analysis of the IEEE 6 bus power system modeled in the PowerWorld Simulator, conducted using the Newton-Raphson method, is shown in Fig. 2.

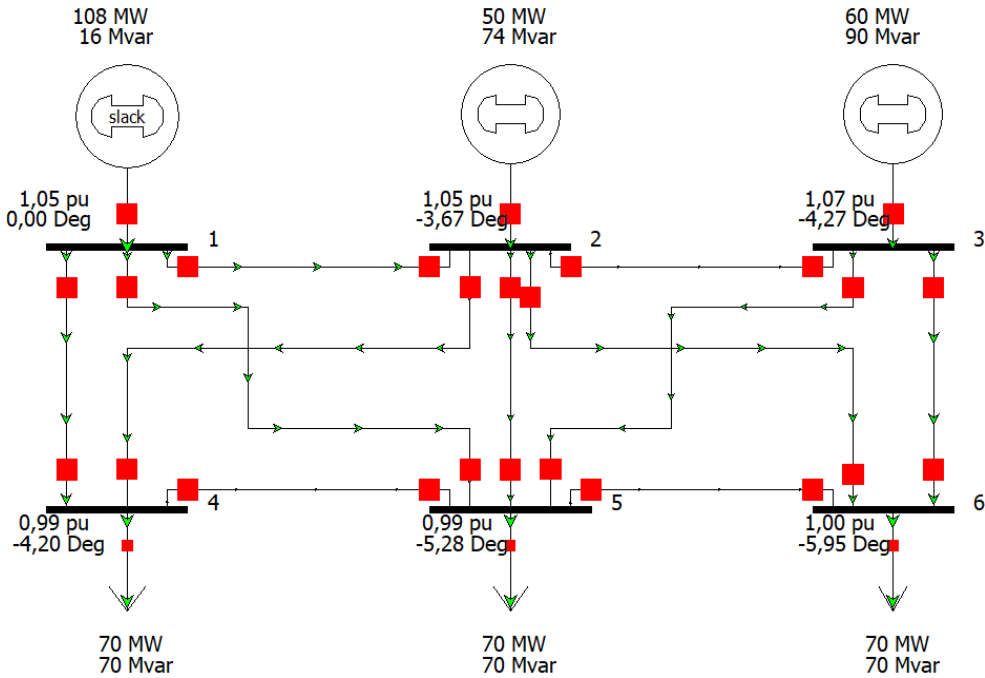


Fig. 2. Simulation results of power flow analysis using the Newton-Raphson method.

3. Results and Discussion

This study will conduct fault analysis on a per-bus basis for buses 1 through 6 of the IEEE 6 bus power system. The simulation results for various fault scenarios are detailed in Tables 4, 5, 6, and 7. These tables can be used to analyze how the system responds to different fault types and how these faults affect the voltage, current, and power values in the system. The voltage magnitudes are given in pu values. This represents normalized values with respect to the nominal value and facilitates comparison of systems with different voltage levels. The angle values are given in degrees and are important indicators for system stability. Large angle differences may indicate that the system is approaching instability. These analyses were performed using the PowerWorld simulator, allowing for quick and effective examination of fault conditions in complex power systems.

Table 4 shows the effects of single line-to-ground faults at each bus in the system. During a fault, the voltage of the faulted phase approaches zero, while the voltages of the other phases increase. For example, when a fault occurs at bus 1, the voltage of phase A becomes zero, while the voltages of phases B and C rise to 1.29516 pu and 1.11105 pu, respectively. Similarly, the angle of the faulted phase changes significantly compared to the other phases. This is a characteristic feature of single line-to-ground faults. Such faults can lead to overloading and potential damage to the equipment.

Table 5 illustrates the phase voltages and angles for each bus in the event of a line-to-line fault. At bus 1, the voltage for phase A is 1.05 pu, and for phases B and C, it is 0.525 pu. This substantial difference in voltages indicates a significant disturbance in voltage balance due to the fault. The phase angles are 0° , -180° , and -180° for phases A, B, and C, respectively, illustrating the phase shift caused by the fault. Such shifts can lead to harmonic distortions and power quality issues in the system.

Table 6 shows the double line-to-ground fault condition. At bus 1, phase A has a voltage of 1.2672 pu, while phases B and C are at 0 pu. The phase angles are 3.52° , -48.81° , and -41.63° for phases A, B, and C, respectively. This substantial discrepancy in voltages and angles highlights the severe imbalance caused by the fault, leading to major energy losses and potential equipment failures.

Table 4. Single line-to-ground (L-G).

Fault Bus	Bus Number	Phase Volt A	Phase Volt B	Phase Volt C	Phase Ang A	Phase Ang B	Phase Ang C
1	1	0	1.29516	1.11105	-1.79	-127.24	134.86
	2	0.28601	1.26616	1.03918	-19.35	-127.39	128.88
	3	0.40035	1.26636	1.04116	-15.34	-126.87	126.67
	4	0.16067	1.2299	1.00935	-25.34	-129.72	130.88
	5	0.20618	1.22515	0.99445	-26.21	-130.29	129.7
	6	0.31088	1.22675	0.9852	-23.26	-129.41	127.41
2	1	0.18558	1.27979	1.07302	7.35	-125.41	133.71
	2	0	1.32507	1.10952	178.52	-131	132.73
	3	0.21743	1.30941	1.0798	-9.84	-129.12	129.58
	4	0.03945	1.26957	1.04126	-31.58	-131.43	133.35
	5	0.08268	1.26309	1.02749	-24.21	-132.07	132.13
	6	0.11365	1.27723	1.03309	-26.18	-132.05	130.81
3	1	0.34773	1.24328	1.05341	4.69	-124.12	131.46
	2	0.25726	1.26976	1.06384	-3.35	-128.57	129.39
	3	0	1.33975	1.13972	-2.59	-131.94	131.65
	4	0.23247	1.21983	1.00773	-6.52	-129.57	130.29
	5	0.13664	1.24171	1.02608	-11.79	-131.89	130.92
	6	0.06701	1.27303	1.05757	-16.37	-133.13	130.73
4	1	0.30631	1.25316	1.08386	3.4	-125.67	132.39
	2	0.29491	1.27452	1.07377	-11.44	-129.07	129.76
	3	0.42596	1.27121	1.0672	-10.6	-128.15	127.33
	4	0	1.27025	1.09479	176.09	-133.86	133.58
	5	0.25236	1.22626	1.01895	-15.47	-131.46	130
	6	0.33145	1.23181	1.01342	-16.63	-130.81	128.06
5	1	0.35045	1.24854	1.0824	4.58	-125.55	132.12
	2	0.33235	1.26769	1.0753	-6.63	-129.08	129.41
	3	0.34731	1.28928	1.09243	-8.95	-129.5	128.63
	4	0.25496	1.22475	1.03252	-7.72	-130.78	130.79
	5	0	1.27801	1.09937	-2.27	-135.36	133.18
	6	0.25189	1.2502	1.04298	-14.52	-132.34	129.38
6	1	0.4123	1.23633	1.06649	4.42	-124.67	131.25
	2	0.32618	1.26363	1.07755	-2.52	-129.14	129.21
	3	0.25591	1.29871	1.11588	-1.84	-130.64	129.36
	4	0.29884	1.21177	1.02042	-4.72	-130.11	129.95
	5	0.21563	1.23031	1.03866	-5.79	-132.41	130.37
	6	0	1.29672	1.1086	1.42	-135.49	132.19

Table 5. Line-to-line (L-L).

Fault Bus	Bus Number	Phase Volt A	Phase Volt B	Phase Volt C	Phase Ang A	Phase Ang B	Phase Ang C
1	1	1.05	0.525	0.525	0	-180	-180
	2	1.05001	0.59849	0.54635	-3.67	-161.3	151.68
	3	1.07002	0.6415	0.60642	-4.27	-154.26	143.78
	4	0.98938	0.52586	0.506	-4.2	-168.02	158.98
	5	0.98545	0.54074	0.51273	-5.28	-165.14	153.44
	6	1.00443	0.58682	0.54487	-5.95	-159.6	145.5
2	1	1.05	0.50272	0.5822	0	-164.29	166.48
	2	1.05001	0.52501	0.52501	-3.67	176.33	176.33
	3	1.07002	0.55371	0.56913	-4.27	-166.38	158.33
	4	0.98938	0.48788	0.50706	-4.2	-178.02	169.86
	5	0.98545	0.48914	0.51357	-5.28	-174.37	164.34
	6	1.00443	0.51143	0.51527	-5.95	-173.95	162.14
3	1	1.05	0.53335	0.65105	0	-149.3	155.28
	2	1.05001	0.52907	0.59922	-3.67	-160.76	156.22
	3	1.07002	0.53501	0.53501	-4.27	175.73	175.73
	4	0.98938	0.49882	0.57399	-4.2	-159.7	154.69
	5	0.98545	0.48415	0.54001	-5.28	-168.56	159.78
	6	1.00443	0.48747	0.52818	-5.95	-177.07	165.86
4	1	1.05	0.53411	0.60268	0	-155.99	158.86
	2	1.05001	0.57787	0.55926	-3.67	-161.49	153.36
	3	1.07002	0.62974	0.62276	-4.27	-153.15	144.21
	4	0.98938	0.49469	0.49469	-4.2	175.8	175.8
	5	0.98545	0.5346	0.53628	-5.28	-162.2	151.72
	6	1.00443	0.57441	0.56075	-5.95	-158.54	145.92

Table 5 (continued). Line-to-line (L-L).

Fault Bus	Bus Number	Phase Volt A	Phase Volt B	Phase Volt C	Phase Ang A	Phase Ang B	Phase Ang C
5	1	1.05	0.53655	0.62641	0	-152.34	156.57
	2	1.05001	0.56753	0.59075	-3.67	-158.16	151.89
	3	1.07002	0.59253	0.59337	-4.27	-158.71	150.2
	4	0.98938	0.51579	0.55324	-4.2	-161.1	154.35
	5	0.98545	0.49273	0.49273	-5.28	174.72	174.72
	6	1.00443	0.53845	0.54102	-5.95	-164.41	152.62
6	1	1.05	0.55548	0.66438	0	-146.23	152.3
	2	1.05001	0.54809	0.6103	-3.67	-157.22	152.74
	3	1.07002	0.54267	0.58782	-4.27	-164.65	157.67
	4	0.98938	0.51699	0.58618	-4.2	-156.11	151.27
	5	0.98545	0.49562	0.55608	-5.28	-163.57	155.47
	6	1.00443	0.50222	0.50222	-5.95	174.05	174.05

Table 6. Double line-to-ground (L-L-G).

Fault Bus	Bus Number	Phase Volt A	Phase Volt B	Phase Volt C	Phase Ang A	Phase Ang B	Phase Ang C
1	1	1.2672	0	0	3.52	-48.81	-41.63
	2	1.20635	0.24159	0.30118	1.14	-137.22	107.67
	3	1.20174	0.34422	0.41693	0.53	-133.91	111.1
	4	1.17916	0.13	0.19565	0.59	-130.07	102.27
	5	1.16838	0.16774	0.2482	-0.18	-132.08	101.23
	6	1.15951	0.25629	0.34666	-0.54	-136.33	104.09
2	1	1.23348	0.15013	0.19225	4	-112.11	136.14
	2	1.28293	0	0	0.31	58.52	-61.48
	3	1.25283	0.18149	0.22515	0.19	-128.9	117.73
	4	1.21996	0.03743	0.06987	0.37	-91.42	100.29
	5	1.20911	0.07164	0.12187	-0.48	-107.46	103.87
	6	1.2183	0.08778	0.14423	-0.99	-125.5	103.16
3	1	1.19699	0.29274	0.36772	3.86	-112.55	131.79
	2	1.22105	0.2146	0.27611	0.45	-119.4	123.95
	3	1.30509	0	0	-0.64	-122.59	117.41
	4	1.16913	0.19903	0.27244	0.3	-114.53	119.38
	5	1.19419	0.12279	0.1807	-0.81	-108.45	113.16
	6	1.22825	0.06074	0.10037	-1.64	-99.42	110.58
4	1	1.21401	0.25135	0.29746	3.18	-120.57	132.79
	2	1.22207	0.24998	0.2869	0.2	-134.77	116.49
	3	1.21242	0.36539	0.42264	-0.27	-132.24	116.56
	4	1.23721	0	0	-1	56.09	-63.91
	5	1.17187	0.2134	0.27333	-1.05	-130.05	111.59
	6	1.16952	0.27854	0.34709	-1.44	-134.09	110.87
5	1	1.20841	0.28685	0.34221	3.08	-118.71	133.91
	2	1.21665	0.27749	0.32462	-0.03	-129.63	121.84
	3	1.23639	0.29461	0.33529	-0.6	-132.66	118.98
	4	1.1755	0.21365	0.26703	-0.42	-124.98	119.93
	5	1.24123	0	0	-2.08	-122.27	117.73
	6	1.1948	0.20968	0.26107	-1.89	-132.7	113.46
6	1	1.19333	0.34599	0.41522	3.24	-116.21	132.28
	2	1.21713	0.27302	0.32576	-0.16	-123.87	125.54
	3	1.25695	0.21325	0.24519	-0.99	-126.61	127
	4	1.16298	0.25478	0.31966	-0.37	-120.23	122.04
	5	1.18464	0.18739	0.23847	-1.55	-118.42	120.13
	6	1.25845	0	0	-2.59	-118.58	121.42

Table 7 presents the three-phase balanced fault condition, which is the most severe type of fault. For bus 1, the phase voltages for all three phases are 0 pu, with phase angles at 90°. At bus 2, all three phase voltages are 0.2651 pu, with phase angles of -10.78°, -130.78°, and 109.22° for phases A, B, and C, respectively. This data indicates symmetrical voltage values but significant differences in phase angles, suggesting a symmetrical disturbance in the system that nonetheless causes phase angle imbalances. Such faults can disrupt the overall stability of the system and necessitate additional balancing measures.

Table 7. Three-phase balanced.

Fault Bus	Bus Number	Phase Volt A	Phase Volt B	Phase Volt C	Phase Ang A	Phase Ang B	Phase Ang C
1	1	0	0	0	90	90	90
	2	0.2651	0.2651	0.2651	-10.78	-130.78	109.22
	3	0.37129	0.37129	0.37129	-7.92	-127.92	112.08
	4	0.16956	0.16956	0.16956	-8.24	-128.24	111.76
	5	0.21563	0.21563	0.21563	-9.88	-129.88	110.12
	6	0.30199	0.30199	0.30199	-11.13	-131.13	108.87
2	1	0.1642	0.1642	0.1642	16.78	-103.22	136.78
	2	0	0	0	178.52	58.52	-61.48
	3	0.19668	0.19668	0.19668	-1.55	-121.55	118.45
	4	0.06166	0.06166	0.06166	6.21	-113.79	126.21
	5	0.10786	0.10786	0.10786	2.37	-117.63	122.37
	6	0.12279	0.12279	0.12279	-4.89	-124.89	115.11
3	1	0.3236	0.3236	0.3236	13.7	-106.3	133.7
	2	0.24183	0.24183	0.24183	6.7	-113.3	126.7
	3	0	0	0	-2.59	-122.59	117.41
	4	0.24339	0.24339	0.24339	6.95	-113.05	126.95
	5	0.16423	0.16423	0.16423	6.5	-113.5	126.5
	6	0.09004	0.09004	0.09004	9.36	-110.64	129.36
4	1	0.25463	0.25463	0.25463	9.69	-110.31	129.69
	2	0.25224	0.25224	0.25224	-6.32	-126.32	113.68
	3	0.37588	0.37588	0.37588	-4.99	-124.99	115.01
	4	0	0	0	176.09	56.09	-63.91
	5	0.24198	0.24198	0.24198	-5.03	-125.03	114.97
	6	0.30544	0.30544	0.30544	-7.62	-127.62	112.38
5	1	0.29328	0.29328	0.29328	11.3	-108.7	131.3
	2	0.28263	0.28263	0.28263	-0.67	-120.67	119.33
	3	0.2952	0.2952	0.2952	-4.17	-124.17	115.83
	4	0.23477	0.23477	0.23477	1.51	-118.49	121.51
	5	0	0	0	-2.27	-122.27	117.73
	6	0.22831	0.22831	0.22831	-5.55	-125.55	114.45
6	1	0.36397	0.36397	0.36397	11.58	-108.42	131.58
	2	0.28473	0.28473	0.28473	4.33	-115.67	124.33
	3	0.21221	0.21221	0.21221	3.18	-116.82	123.18
	4	0.28454	0.28454	0.28454	4.81	-115.19	124.81
	5	0.21495	0.21495	0.21495	4.7	-115.3	124.7
	6	0	0	0	1.42	-118.58	121.42

Several critical observations can be derived from the analysis of these tables. Firstly, the bus where the fault occurs experiences the lowest voltage values. Secondly, the three-phase balanced fault generally causes the most severe voltage drops. Thirdly, as we move away from the fault location, voltage values tend to approach nominal values. Lastly, phase angles also show significant changes during fault conditions, which can affect power flows.

Figs. 3-14, which depict the system's response to faults at buses 4, 5, and 6. Fig. 3 illustrates the rotor angle dynamics of the generators when a fault occurs at bus 4. The rotor angle, which represents the angular position of the rotor in relation to a reference, is critical for assessing system stability. As can be seen from the graph, there is a sudden increase in the rotor angle during the fault, and the system undergoes an oscillation process to reach a stable state. This indicates that the system stability is disturbed, and it requires time to regain a stable operating condition after the fault.

Fig. 4 depicts the power flow changes in the system during the fault at bus 4. This graph is essential for understanding the immediate impact on power delivery and the system's ability to maintain stable power flows under fault conditions. During the fault, there are significant fluctuations in the active powers, but the system undergoes a period of oscillation to reach a stable condition. These power fluctuations indicate the disturbance in the system stability.

Fig. 5 presents the current levels in the system when bus 4 experiences a fault. During the fault, there are sudden increases in the currents, and the system experiences an oscillation process. These current variations suggest that the system stability is disturbed, and it requires time to regain a stable operating state. Analyzing these currents is crucial for the design and coordination of protective devices.

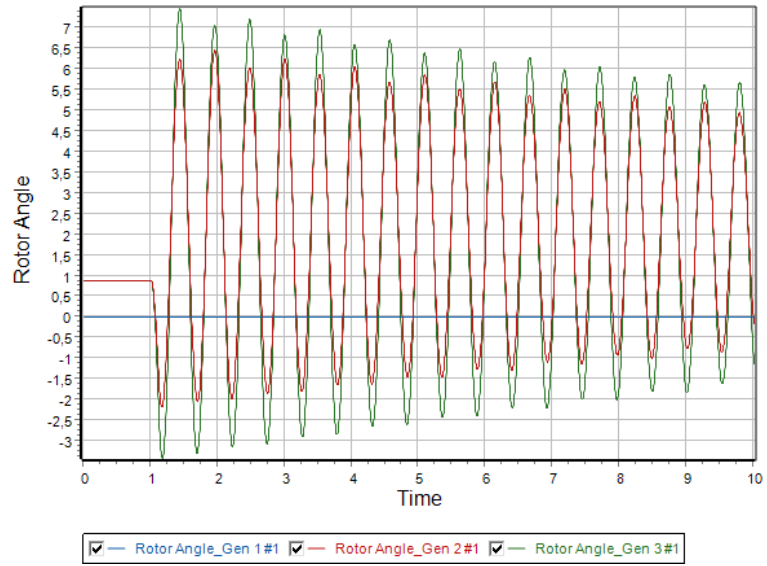


Fig. 3. Plot of rotor angle for fault at bus 4.

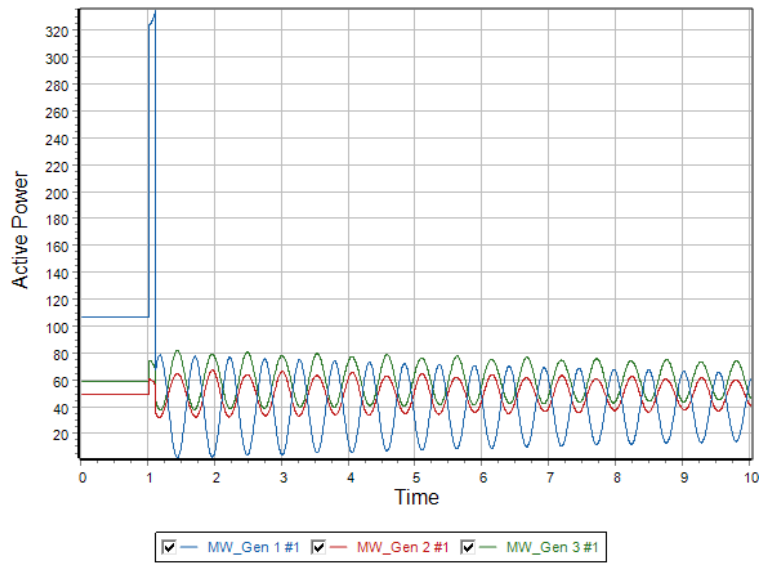


Fig. 4. Plot of active power for fault at bus 4.

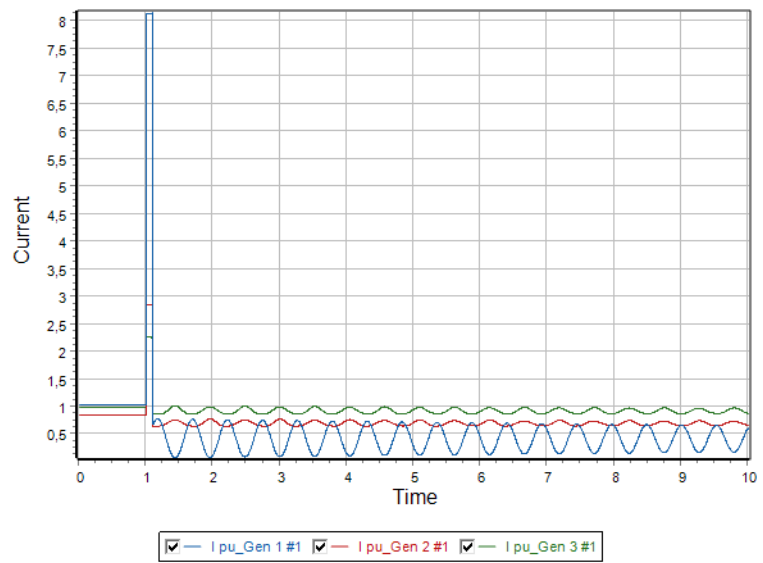


Fig. 5. Plot of current for fault at bus 4.

Fig. 6 shows the changes in the generator phase voltages when bus 4 is in a faulty condition. During the fault, there are sudden drops in the voltages, and the system undergoes an oscillation process. These voltage fluctuations indicate the disturbance in the system stability, and the system needs time to return to a stable condition. This graph highlights the voltage sags and subsequent recovery, providing insights into the voltage stability and resilience of the system during fault conditions.

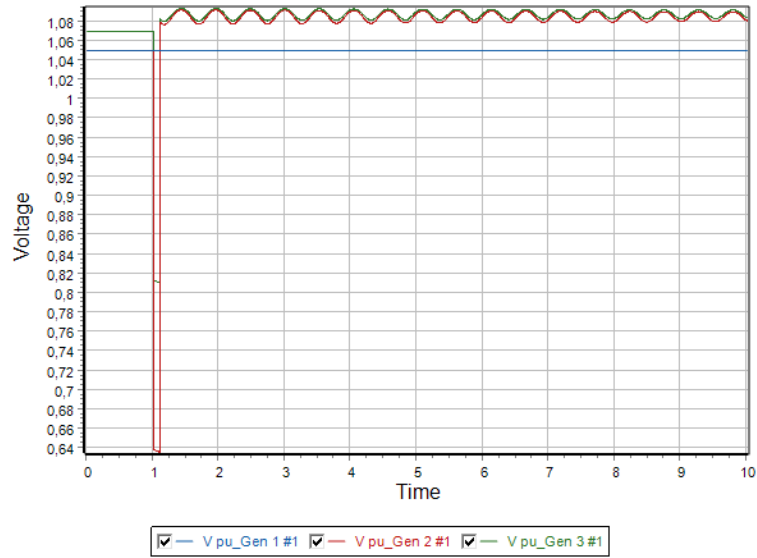


Fig. 6. Plot of voltage for fault at bus 4.

Fig. 7 depicts the variation of the rotor angle of the generators when bus 5 is in a faulty condition. Similar to the case of bus 4, there is a sudden increase in the rotor angle during the fault, and the system experiences an oscillation process to reach a stable state. This suggests that the system stability is disturbed, and it requires time to regain a stable operating condition after the fault.

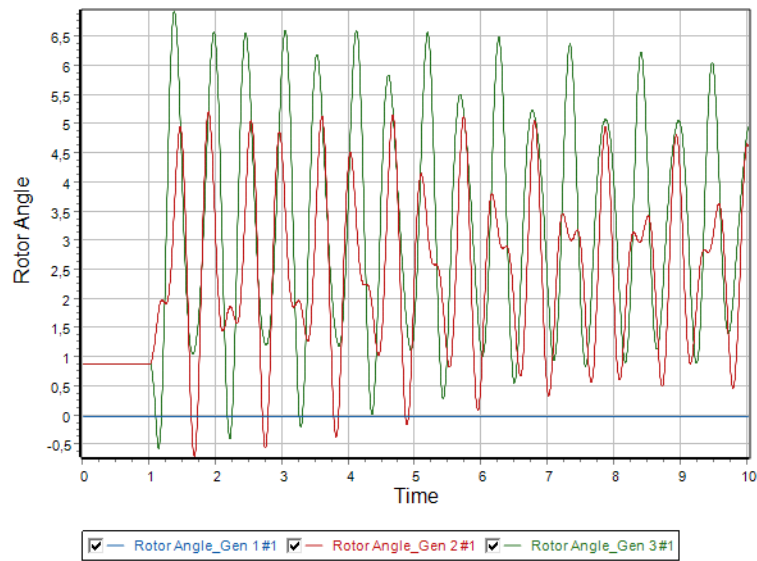


Fig. 7. Plot of rotor angle for fault at bus 5.

Fig. 8 represents the power flow variations due to a fault at bus 5. During the fault, there are significant fluctuations in the active powers, but the system undergoes a period of oscillation to reach a stable condition. These power fluctuations indicate the disturbance in the system stability. This graph helps in understanding the redistribution of power and the potential for overloads or underloads in different parts of the network.

Fig. 9 for a fault at bus 5 shows the fault currents and their behavior over time. During the fault, there are sudden increases in the currents, and the system experiences an oscillation process. These current variations suggest that the system stability is disturbed, and it requires time to regain a stable operating state. This information is vital for the accurate setting of overcurrent protection devices and ensuring they operate correctly during faults.

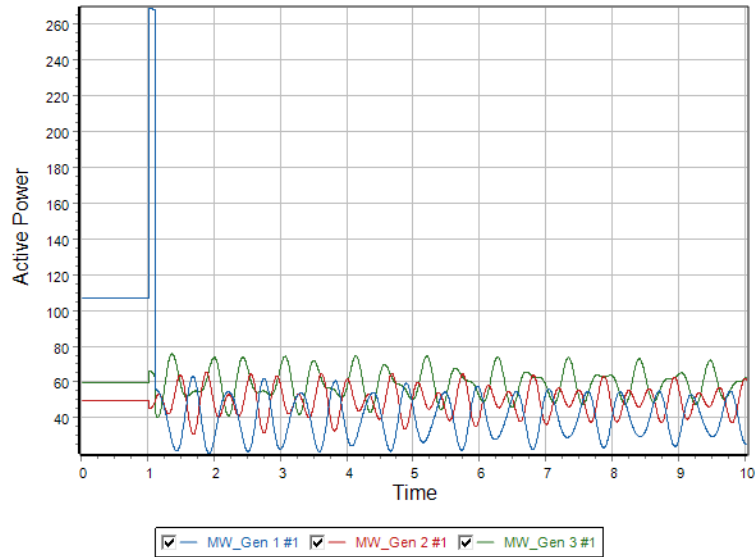


Fig. 8. Plot of active power for fault at bus 5.

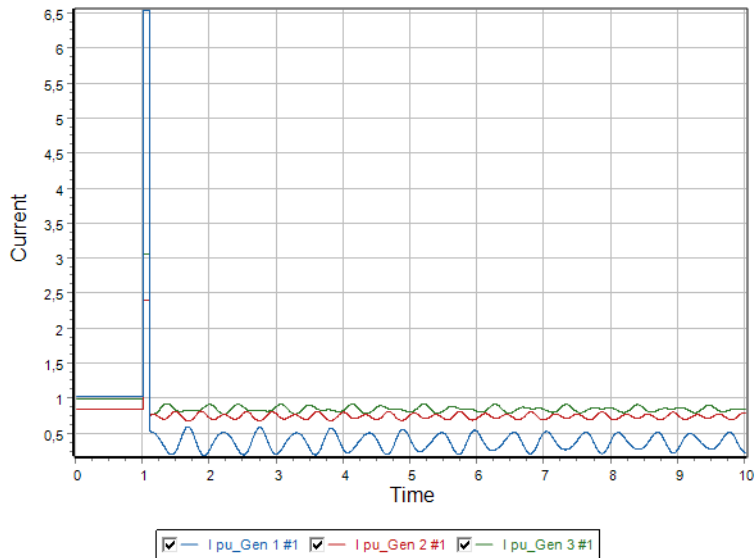


Fig. 9. Plot of current for fault at bus 5.

Fig. 10 illustrates the voltage response throughout the system when bus 5 is faulted. During the fault, there are sudden drops in the voltages, and the system undergoes an oscillation process. These voltage fluctuations indicate the disturbance in the system stability, and the system needs time to return to a stable condition. This graph helps in identifying critical voltage dips and the recovery process, crucial for voltage stability analysis and corrective actions.

The rotor angle dynamics for a fault at bus 6 are shown in Fig. 11. As in the previous cases, there is a sudden increase in the rotor angle during the fault, and the system experiences an oscillation process to reach a stable state. This indicates that the system stability is disturbed, and it requires time to regain a stable operating condition after the fault. This graph provides data on the generator stability and synchronization post-fault, essential for maintaining overall system stability.

Fig. 12 presents the power flow changes resulting from a fault at bus 6. During the fault, there are significant fluctuations in the active powers, but the system undergoes a period of oscillation to reach a stable condition. These power fluctuations indicate the disturbance in the system stability. This graph indicates the impact on power distribution and can highlight any potential issues with power balancing in the system.

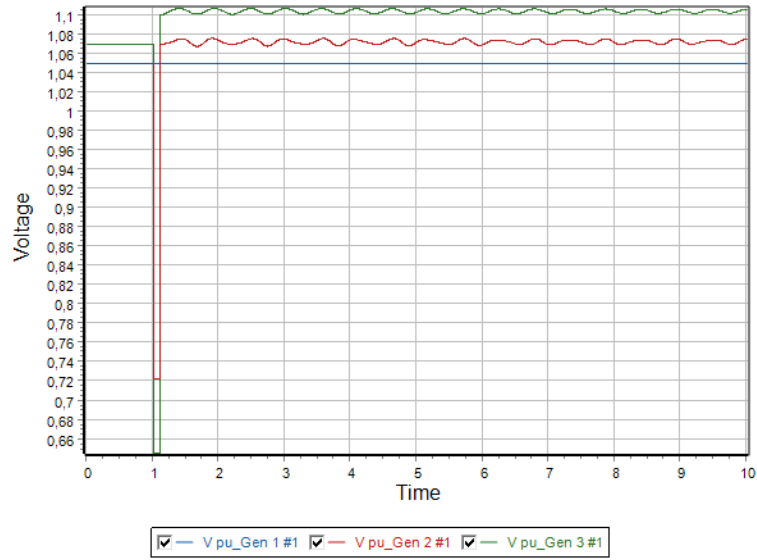


Fig. 10. Plot of voltage for fault at bus 5.

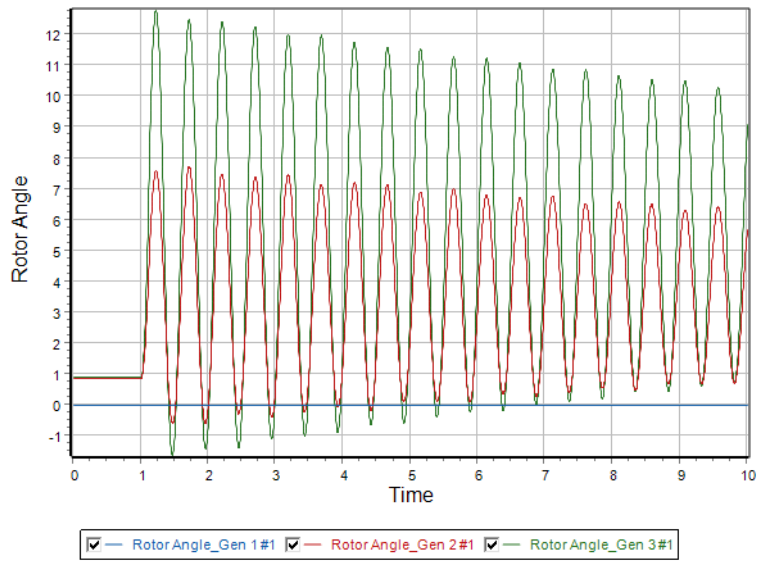


Fig. 11. Plot of rotor angle for fault at bus 6.

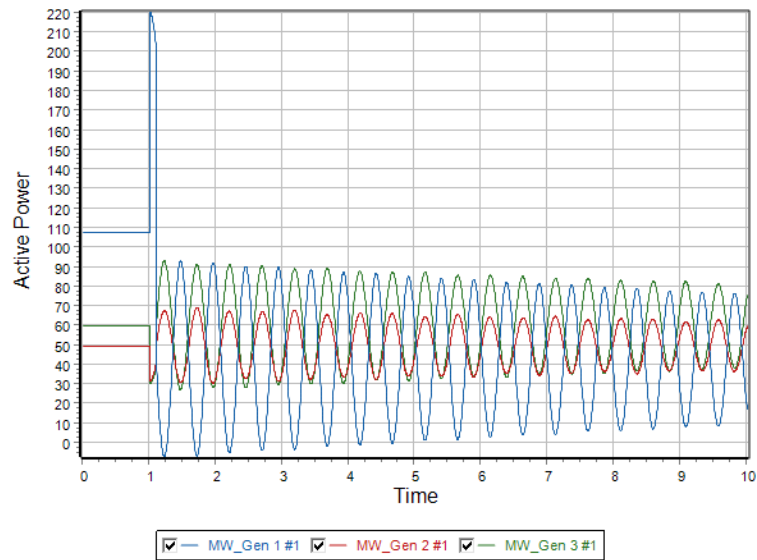


Fig. 12. Plot of active power for fault at bus 6.

The current levels during a fault at bus 6 are depicted in Fig. 13. During the fault, there are sudden increases in the currents, and the system experiences an oscillation process. These current variations suggest that the system stability is disturbed, and it requires time to regain a stable operating state. Analyzing these currents helps in understanding the severity of the fault and the required settings for protection equipment.

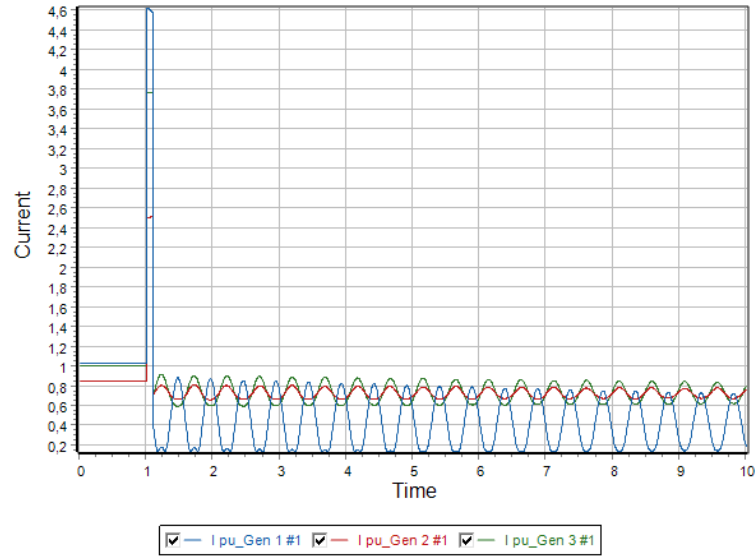


Fig. 13. Plot of current for fault at bus 6.

Fig. 14 shows the voltage variations across the system when bus 6 is faulted. During the fault, there are sudden drops in the voltages, and the system undergoes an oscillation process. These voltage fluctuations indicate the disturbance in the system stability, and the system needs time to return to a stable condition. This graph is crucial for evaluating the system’s voltage support mechanisms and the effectiveness of voltage control strategies.

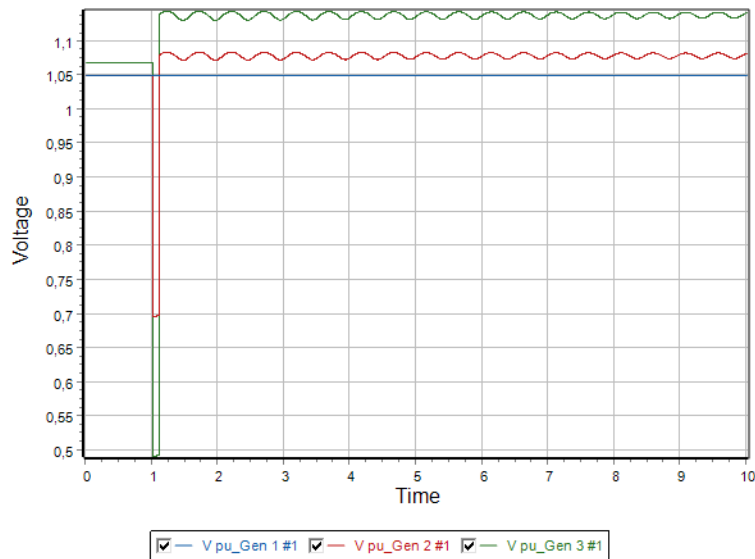


Fig. 14. Plot of voltage for fault at bus 6.

Each of these figures provides critical insights into different aspects of power system behavior under fault conditions, aiding in the comprehensive analysis and design of robust power systems. The detailed study of these graphs helps in improving fault detection, isolation, and system recovery strategies, ensuring reliable and stable operation.

The results align with established power system theory, demonstrating that three-phase balanced faults pose the most significant threat to stability due to substantial voltage deviations and phase angle shifts, while line-to-ground faults, the most frequent type, cause significant voltage instability at the faulted bus. Line-to-line faults primarily impact phase voltages, creating asymmetrical disturbances, and double line-to-ground faults exhibit complex dynamics, combining characteristics of both line-to-ground and line-to-line faults. The findings are consistent with previous research on transient stability using PowerWorld

Simulator, emphasizing the importance of fault location, fault type, and system configuration in determining overall stability and reliability.

The analysis underscores the critical role of fault location, with buses closer to the fault experiencing more pronounced effects. This highlights the need for localized protective measures that can quickly isolate faults and minimize their impact. The observed rotor angle dynamics, power flow changes, current variations, and voltage fluctuations provide critical insights into system stability, informing the design of control strategies and protection schemes. The study's findings can be used to develop and validate techniques that enhance power network resilience, such as power system stabilizers, robust power flow control strategies, and accurate settings for overcurrent protection devices. These insights are crucial for designing voltage support mechanisms and improving system resilience against disturbances.

Despite the valuable insights provided, the study is based on a simplified model and assumes ideal fault conditions. Future research should focus on extending this analysis to larger, more realistic power systems, investigating the impact of varying system parameters, and evaluating the effectiveness of different protection schemes. Exploring advanced control strategies, such as Flexible Alternating Current Transmission System (FACTS) devices, and the integration of renewable energy sources, along with their impact on transient stability, warrants further investigation. This research contributes to a broader understanding of power system dynamics and can inform the design and operation of more robust and efficient power systems capable of withstanding disturbances and maintaining stability under a wide range of conditions.

4. Conclusion

This research has conducted a comprehensive transient analysis of the IEEE 6 bus power system under various fault conditions using the PowerWorld Simulator. The study systematically investigated the system's dynamic behavior in response to single line-to-ground, line-to-line, double line-to-ground, and three-phase balanced faults at different bus locations. The analysis revealed distinct patterns of transient response for each fault type, highlighting the importance of understanding the specific characteristics of each fault scenario.

The results demonstrate that three-phase balanced faults, while less frequent, pose the most significant threat to system stability, causing substantial voltage deviations and phase angle shifts. Line-to-ground faults, although less severe, can still lead to voltage instability at the faulted bus. Line-to-line faults primarily impact phase voltages, creating asymmetrical disturbances that propagate through the network. Double line-to-ground faults exhibit complex transient dynamics, combining characteristics of line-to-line and line-to-ground faults, and testing the system's resilience and control mechanisms. The study underscores the necessity for robust protective measures and control strategies to mitigate the adverse effects of these faults. The findings highlight the importance of fault location, fault type, and system configuration in determining the overall stability and reliability of the power system. This research contributes to the broader understanding of power system dynamics and can be used to develop and validate control strategies, protection schemes, and mitigation techniques that can be applied to larger-scale power systems with similar characteristics.

Future research can investigate how varying system parameters like loading levels, generator inertia, and transmission line characteristics impact transient stability in power systems. Additionally, there is a need to evaluate different protection schemes and relaying strategies to determine their effectiveness in isolating faults and maintaining system stability. Exploring advanced control strategies, such as using FACTS devices, could also enhance power flow regulation and system robustness.

References

- [1] P. Bhatt and S. Kumar, "Comprehensive assessment of fault current contribution in smart distribution grid with solar photovoltaic," *Technology and Economics of Smart Grids and Sustainable Energy*, vol. 2, no. 1, 2017. <https://doi.org/10.1007/s40866-017-0023-8>
- [2] M. Begum, M. Alam, and K. Muttaqi, "Analytical expressions for characterising voltage dips and phase-angle jumps in electricity networks," *IET Generation, Transmission & Distribution*, vol. 13, no. 1, p. 116-126, 2018. <https://doi.org/10.1049/iet-gtd.2018.6348>
- [3] R. Salim, K. Salim, and A. Bretãs, "Further improvements on impedance-based fault location for power distribution systems," *IET Generation, Transmission & Distribution*, vol. 5, no. 4, p. 467, 2011. <https://doi.org/10.1049/iet-gtd.2010.0446>
- [4] D. Zhang, "An alternative approach to analyze un-symmetrical faults in power systems," *TENCON 2009 - 2009 IEEE Region 10 Conference*, Singapore, 2009, pp. 1-6. <https://doi.org/10.1109/tencon.2009.5396193>

- [5] Y. Altınok, M. Lüy, N. A. Metin, S. Görgülü Balcı, and F. Acar, "Sustainable grids: Smart meter solutions for efficient energy measurement," *International Scientific and Vocational Studies Journal*, vol. 8, no. 1, pp. 49–64, 2024. <https://doi.org/10.47897/bilmes.1485662>
- [6] K. Mets, J. A. Ojea, and C. Develder, "Combining power and communication network simulation for cost-effective smart grid analysis," *IEEE Communications Surveys & Tutorials*, vol. 16, no. 3, pp. 1771–1796, 2014. <https://doi.org/10.1109/surv.2014.021414.00116>
- [7] A. Çifci, "Use of PowerWorld simulator in learning power flow analysis: A computer-aided visualization tool," *The Journal of Graduate School of Natural and Applied Sciences of Mehmet Akif Ersoy University*, vol. 13, no. 2, pp. 281–291, Dec. 2022. <https://doi.org/10.29048/makufebed.1153316>
- [8] A. Jain, A. Mani, and A. S. Siddiqui, "Simulation of a microgrid with OpenDSS an open-source software package," *Lecture Notes in Electrical Engineering*, pp. 513–529, Jan. 2023. https://doi.org/10.1007/978-981-19-6383-4_42
- [9] C. Zuo, B. Wang, M. Zhang, M. A. Khanwala, and S. Dang, "Power flow analysis using PowerWorld: A comprehensive testing report," in *2015 International Conference on Fluid Power and Mechatronics (FPM)*, 2015.
- [10] H. Huang, Z. Mao, M. R. Narimani, and K. R. Davis, "Toward efficient wide-area identification of multiple element contingencies in power systems," in *2021 IEEE Power & Energy Society Innovative Smart Grid Technologies Conference (ISGT)*, 2021.
- [11] H. Wen, "Power flow analysis of 110kV power supply system based on PowerWorld," *Journal of Physics. Conference Series*, vol. 2495, no. 1, p. 012025, May 2023. <https://doi.org/10.1088/1742-6596/2495/1/012025>
- [12] X. Li, C. Liu, P. Guo, S. Liu, and J. Ning, "Deep learning-based transient stability assessment framework for large-scale modern power system," *International Journal of Electrical Power & Energy Systems*, vol. 139, p. 108010, Jul. 2022. <https://doi.org/10.1016/j.ijepes.2022.108010>
- [13] R. Kaur and D. Kumar, "Transient stability improvement of IEEE 9 bus system using power world simulator," *MATEC Web of Conferences*, vol. 57, p. 01026, 2016. <https://doi.org/10.1051/mateconf/20165701026>
- [14] M. Mahasathyavathi, R. Balasubramani, and L. Jeeva, "Load frequency control for multi-area power system using PWS," *International Journal of Research in Advent Technology*, vol. 7, no. 4, p. 212-219, 2019. <https://doi.org/10.32622/ijrat.732019187>
- [15] S. Kim and T. Overbye, "Optimal subinterval selection approach for power system transient stability simulation," *Energies*, vol. 8, no. 10, p. 11871-11882, 2015. <https://doi.org/10.3390/en81011871>
- [16] P. Demetriou, M. Asprou, J. Quirós-Tortós, and E. Kyriakides, "Dynamic IEEE test systems for transient analysis," *IEEE Systems Journal*, vol. 11, no. 4, p. 2108-2117, 2017. <https://doi.org/10.1109/jsyst.2015.2444893>
- [17] A. Anuar, M. A. A. Wahab, S. N. M. Arshad, M. I. F. Romli, A. H. A. Bakar, and M. A. A. Bakar, "Transient stability for IEEE 14 bus power system using power world simulator," *J. Phys. Conf. Ser.*, vol. 1432, no. 1, p. 012009, 2020. <https://doi.org/10.1088/1742-6596/1432/1/012009>
- [18] N. Anwar, A. H. Hanif, H. F. Khan, and M. F. Ullah, "Transient stability analysis of the IEEE-9 bus system under multiple contingencies," *Eng. Technol. Appl. Sci. Res.*, vol. 10, no. 4, pp. 5925–5932, 2020. <https://doi.org/10.48084/etasr.3273>
- [19] K. Patel, "Transient stability analysis and tuning of power system stabilizer for three machine nine bus system using frequency response approach," in *2020 International Conference on Advances in Computing and Communication Engineering (ICACCE)*, 2020.
- [20] G. M. Tina, G. Maione, S. Licciardello, and D. Stefanelli, "Comparative technical-economical analysis of transient stability improvements in a power system," *Appl. Sci. (Basel)*, vol. 11, no. 23, p. 11359, 2021. <https://doi.org/10.3390/app112311359>
- [21] P. V. Rajesh Varma, M. K. Kar, and A. K. Singh, "Transient analysis of a standard IEEE-9 bus power system using power world simulator," in *Advances in Smart Grid Automation and Industry 4.0*, Singapore: Springer Singapore, 2021, pp. 233–243. https://doi.org/10.1007/978-981-15-7675-1_22

- [22] G. M. Tina, G. Maione, and S. Licciardello, "Evaluation of technical solutions to improve transient stability in power systems with wind power generation," *Energies*, vol. 15, no. 19, p. 7055, 2022. <https://doi.org/10.3390/en15197055>
- [23] N. A. Salim, H. Mohamed, M. E. S. Bin Ensnat, and Z. M. Yasin, "System transient stability due to various contingency using power world simulator," in *2023 IEEE 3rd International Conference in Power Engineering Applications (ICPEA)*, 2023.
- [24] H. Saadat, *Power System Analysis*, 3rd ed., Alexandria: PSA Publishing LLC, 2010.